Title

Microbial Respiration and Formate Oxidation as Metabolic Signatures of Inflammation-Associated Dysbiosis

Journal

Cell Host & Microbe, 21(2)

ISSN

1931-3128

Authors

Hughes, Elizabeth R
Winter, Maria G
Duerkop, Breck A
et al.

Publication Date

2017-02-01

DOI

10.1016/j.chom.2017.01.005

Peer reviewed

HHS Public Access

Author manuscript

Cell Host Microbe. Author manuscript; available in PMC 2018 February 08.

Published in final edited form as:

Cell Host Microbe. 2017 February 08; 21(2): 208–219. doi:10.1016/j.chom.2017.01.005.

Microbial respiration and formate oxidation as metabolic signatures of inflammation-associated dysbiosis

Elizabeth R. Hughes[1,*], **Maria G. Winter**[1,*], **Breck A. Duerkop**[2], **Luisella Spiga**[1], **Tatiane Furtado de Carvalho**[3], **Wenhan Zhu**[1], **Caroline C. Gillis**[1], **Lisa Büttner**[1], **Madeline P. Smoot**[1], **Cassie L. Behrendt**[2], **Sara Cherry**[4], **Renato L. Santos**[3], **Lora V. Hooper**[2,5], and **Sebastian E. Winter**[1]

[1]Department of Microbiology, UT Southwestern Medical Center, Dallas, TX 75390, USA

[2]Department of Immunology, UT Southwestern Medical Center, Dallas, TX 75390, USA

[3]Departamento de Clínica e Cirurgia Veterinárias, Escola de Veterinária, Universidade Federal de Minas Gerais, Belo Horizonte, Brazil

[4]Department of Microbiology, University of Pennsylvania School of Medicine, Philadelphia, PA 19104, USA

[5]Howard Hughes Medical Institute, UT Southwestern Medical Center, Dallas, TX 75390, USA

SUMMARY

Intestinal inflammation is frequently associated with an alteration of the gut microbiota, termed dysbiosis, which is characterized by a reduced abundance of obligate anaerobic bacteria and an expansion of Proteobacteria such as commensal *E. coli*. The mechanisms enabling the outgrowth of Proteobacteria during inflammation are incompletely understood. Metagenomic sequencing revealed bacterial formate oxidation and aerobic respiration to be overrepresented metabolic pathways in a chemically-induced murine model of colitis. Dysbiosis was accompanied by increased formate levels in the gut lumen. Formate was of microbial origin since no formate was detected in germ-free mice. Complementary studies using commensal *E. coli* strains as model organisms indicated that formate dehydrogenase and terminal oxidase genes provided a fitness advantage in murine models of colitis. *In vivo*, formate served as electron donor in conjunction with oxygen as the terminal electron acceptor. This work identifies bacterial formate oxidation and oxygen respiration as metabolic signatures for inflammation-associated dysbiosis.

Corresponding Author and Lead Contact: Sebastian.Winter@UTSouthwestern.edu.
*Authors contributed equally

SUPPLEMENTAL INFORMATION

Supplemental Information, including Supplemental Experimental Procedures and additional figures, can be found with this article online.

AUTHOR CONTRIBUTIONS

Conceptualization, E.R.H., M.G.W., L.V.H., S.C., R.L.S., and S.E.W.; Methodology, M.G.W., E.R.H., and L.S.; Software, B.A.D. and W.Z.; Investigation, E.R.H., M.G.W., W.Z., L.S., T.F.C., C.G., L.B., C.L.B., M.P.S. and R.S. Writing, all authors; Supervision, S.E.W., M.G.W., B.A.D., L.V.H., S.C., and R.L.S.

INTRODUCTION

The most abundant bacterial populations of the gut microbiota are obligate anaerobic bacteria belonging to the phyla Bacteroides (class Bacteroidia) and Firmicutes (class Clostridia), while members of the phyla Actinobacteria, Fusobacteria, Verrucomicrobia, and facultative anaerobic Proteobacteria typically constitute minor populations in healthy adults. In the large intestine, bacterial communities compete for limiting carbon and energy sources, mostly complex polysaccharides of dietary or host origin (reviewed in (Cockburn and Koropatkin, 2016; Fischbach and Sonnenburg, 2011; Flint et al., 2012; Koropatkin et al., 2012; Martens et al., 2014)). The ability to efficiently degrade and ferment a variety of complex polysaccharides is a major driving force for microbial colonization of the gut lumen (Eilam et al., 2014). Changes in the host's diet can lead to alterations of composition of the gut microbiota, however these changes are limited to the species level and the overall dominance of obligate anaerobic bacteria over facultative anaerobes is conserved (Faith et al., 2011; Sonnenburg et al., 2010; Sonnenburg and Backhed, 2016; Wu et al., 2011).

In contrast, intestinal inflammation is accompanied by disruption of the gut microbiota composition (dysbiosis). A common feature of bacterial dysbiosis is an expansion of the population of Proteobacteria, in particular members of the Enterobacteriaceae family (reviewed in (Shin et al., 2015; Winter et al., 2013a)). On a population level, this phenomenon was first noted in patients with inflammatory bowel disease (IBD) (Baumgart et al., 2007; Frank et al., 2007; Giaffer et al., 1991; Seksik et al., 2003). Similar observations were made in patients with HIV enteropathy (Vujkovic-Cvijin et al., 2013), parasitic infections (Raetz et al., 2013), animal models of intestinal inflammation (Lupp et al., 2007), and animal models of infection with enteric pathogens (Stecher et al., 2007). The complexity of the gut microbiota and the close association between mucosal inflammation and dysbiosis have been major impediments for investigating the mechanisms underlying the phylum-level changes in microbiota composition during episodes of inflammation. Here, we performed a metagenomic analysis on microbial community changes in response to inflammatory insults to determine which bacterial metabolic pathways could provide a fitness advantage during inflammatory conditions. To assess functional consequences, metagenomic analysis was complemented by a reductionist approach focusing on bacterial model organisms. Our data suggest that formate oxidation and respiration are important pathways contributing to the outgrowth of Enterobacteriaceae in the inflamed intestinal tract.

RESULTS

Metagenomic sequencing of the gut microbiota reveals changes in the metabolic landscape in the lumen of the inflamed intestine

We performed metagenomic shotgun sequencing on the native cecal microbiota in a chemically-induced murine model of colitis (dextran sulfate sodium [DSS]-induced colitis; Fig. S1A). Induction of inflammation was accompanied by changes in the composition of the microbial community (Fig. 1A and B), as predicted by the lowest common ancestor algorithm using the NCBI database (MEGAN5) (Huson et al., 2007). A relative expansion of the phyla Proteobacteria (in particular, Alphaproteobacteria and members of the

Enterobacteriaceae family members), Deferribacteres (*Mucispirillum* sp.), and *Verrucomicrobia*/*Chlamydia* (Verrucomicrobiaceae family) was noted, consistent with previous observations (Berry et al., 2012; Lupp et al., 2007; Nagalingam et al., 2011). We next analyzed the potential metabolic functions encoded by the microbiome using the SEED classification (Fig. 1C and S2, complete dataset deposited at the European Nucleotide Archive, accession number PRJEB15095). Application of the Analysis of Similarity algorithm to a Bray Curtis dissimilarity matrix revealed a significant change in the overall genetic content of microbial communities in homeostatic and inflammatory conditions (R = 0.428, P = 0.008). Notably, an increased abundance of genes encoding for components of the electron transport chain, such as respiratory dehydrogenases, terminal oxidases, and terminal reductases, was associated with DSS-induced inflammation (Fig. 1C, S1F and S2).

Contribution of molybdopterin cofactor-dependent processes to fitness of Enterobacteriaceae in the murine gut

To investigate the mechanisms that drive the expansion of the Enterobacteriaceae population during bouts of inflammation, we focused on *E. coli* as a model organism. Experimental introduction of the human commensal *E. coli* strain Nissle 1917 (EcN) by orogastric gavage resulted in low levels of intestinal colonization in the absence of inflammation (Fig. 2A-C and S3A-E). Administration of DSS was accompanied by weight loss and acute inflammation of the large intestine (Fig. 2A and S3A-E). To study the metabolic pathways that promote fitness of *E. coli* under inflammatory conditions, we introduced EcN after the onset of disease, i.e. after four days of DSS treatment (Fig. S1B and S3A). Several enzymes identified in the metagemomic analysis including nitrate reductases, trimethylamine *N*-oxide (TMAO) reductases, and formate dehydrogenases contain a molybdopterin cofactor (MoCo) in their active site (reviewed in (Cheng and Weiner, 2007; Cole and Richardson, 2008; Leimkuhler and Iobbi-Nivol, 2016; Magalon and Mendel, 2008; Sawers et al., 2004)). To determine the contribution of MoCo-dependent enzymes to gut colonization, groups of mice were intragastrically inoculated with the EcN wild-type strain (WT) or an isogenic mutant defective for the biosynthesis of the MoCo (Δ*moaA* mutant). Five days after inoculation the bacterial load in the large intestinal content was determined by plating on selective media (Fig. 2B and C). The EcN WT robustly colonized the large intestine while the Δ*moaA* mutant was recovered in significantly lower numbers (42-fold in the colon; 64-fold in the cecum).

To explore whether MoCo-dependent enzymes might enhance fitness of members of the Enterobacteriaceae family, we analyzed three murine commensals. *E. coli* SL1, *K. oxytoca* CG57, and *E. cloacae* CG36 were originally isolated from our mouse colony. Deletion of the *moaA* gene abolished activity of the MoCo-dependent nitrate reductases (Fig. S3F). Groups of DSS-treated mice were orogastrically inoculated with an equal mixture of the respective WT and an isogenic Δ*moaA* mutant (competitive fitness assay; Fig. S1B). After five days, the bacterial load in the colon and cecum content was determined and the ratio of the two populations calculated (competitive index) (Fig. 2D and S3G). The murine *E. coli, K. oxytoca*, and *E. cloacae* WT strains outcompeted the isogenic *moaA* mutants in the DSS colitis model. Similarly, the WT of the human commensal EcN outcompeted an isogenic Δ*moaA* mutant (Fig. 2D, 3A, S3G and S4A). In contrast, the EcN WT and the Δ*moaA*

mutant displayed equal fitness in the absence of inflammation (Fig. 3A and S4A), consistent with our previous findings (Winter et al., 2013b). Collectively, these experiments demonstrate that MoCo biosynthesis is required for full fitness of Enterobacteriaceae family members in the inflamed gut but is dispensable for growth under homeostatic conditions.

Contribution of anaerobic respiratory pathways to *E. coli* growth in the intestinal tract

We have recently shown that inflammation-derived nitrate promotes growth of *E. coli* through anaerobic nitrate respiration (Winter et al., 2013b). Accordingly, an EcN mutant lacking all three nitrate reductases (Δ*narG* Δ*narZ* Δ*napA* mutant; NR mutant) is outcompeted by the EcN WT in the DSS colitis model (6-fold) (Fig. 3A and S4A). Intriguingly, the phenotype of the nitrate reductase-deficient mutant was significantly smaller than the phenotype of the Δ*moaA* mutant (6.3-fold vs. 31-fold), raising the possibility that other MoCo-dependent enzymes might contribute to growth of *E. coli* in the inflamed gut.

The *E. coli* genome harbors two DMSO reductases encoded by the *dmsABC* and *ynfFGH* operons, and three TMAO reductases encoded by the *torCAD*, *torYZ*, and *yedYZ* operons (Blattner et al., 1997)(Fig. S1F). We therefore generated a mutant of EcN carrying non-polar unmarked deletions in *narG napA narZ torA torZ yedY dmsA* and *ynfF* (Δ8 mutant). *In vitro*, this mutant did not display a generalized growth defect when cultured aerobically or anaerobically in minimal media (Fig. S4B and C). Consistent with the known functions of anaerobic respiratory enzymes (reviewed in (Unden et al., 2014)), the EcN WT outcompeted the Δ8 mutant during anaerobic growth when alternative electron acceptors were added to the media (Fig. S4D). In the DSS colitis model, the competitive disadvantage of the Δ8 mutant was comparable to the Δ*narG* Δ*narZ* Δ*napA* mutant (Fig. 3A and S4A), suggesting that TMAO and DMSO respiration might be dispensable for fitness in this particular animal model of colitis. Reduction of nitrite by the MoCo-independent Nrf enzyme did not provide a significant fitness advantage in this model (Δ8 *nrfA* mutant). Furthermore, the Δ8 mutant outcompeted the Δ*moaA* mutant (7-fold; Fig. 3A and S4A), prompting us to investigate MoCo-dependent enzymes other than terminal reductases.

Respiratory formate dehydrogenases enhance fitness of *E. coli* in the inflamed intestine

E. coli produces three MoCo-dependent formate dehydrogenases: formate dehydrogenase-N (FDN), formate dehydrogenase-O (FDO), and formate dehydrogenase-H, encoded by *fdnGHI*, *fdoGHI*, and *fdhF*, respectively (Sawers et al., 2004). FDN and FDO convert formate to CO_2 and 2 protons; the electrons liberated from this reaction are shuttled to the respiratory chain (Ruiz-Herrera et al., 1969; Scott and DeMoss, 1976; Wrigley and Linnane, 1961). In contrast, formate dehydrogenase-H is part of the fermentative formate hydrogenlyase complex (Tasman and Pot, 1935) and was excluded from further analysis. To test whether FDN and FDO support *E. coli* growth in the inflamed gut, we introduced mutations in the major subunits of FDN and FDO in the Δ8 mutant. This Δ8 Δ*fdnG fdoG* mutant was outcompeted by the EcN WT in the DSS colitis model (Fig. 3A, Fig. S4A), recapitulating the phenotype of the Δ*moaA* mutant. Furthermore, in a separate competition experiment, the Δ*moaA* mutant and the Δ8 Δ*fdnG fdoG* mutant were recovered in

comparable numbers. This data suggested that formate dehydrogenases enhance fitness of *E. coli* during DSS-induced colitis.

Next, we re-analyzed our metagenomics experiment to specifically determine whether increased abundance of formate dehydrogenase operons correlated with gut inflammation. Sequencing reads were mapped to representative *fdoGHI* and *fdnGHI* operons (Fig. 3B). Virtually no reads mapped to the formate dehydrogenase operons in mock-treated mice. In contrast, a significant portion of the reads mapped to these operons in DSS-treated animals.

To directly test the idea that formate dehydrogenases promote fitness of *E. coli* in the inflamed gut, we generated an EcN mutant lacking FDN and FDO activity (Δ*fdnG fdoG* mutant). This strain was unable to utilize formate *in vitro* (Fig. S5A and B). In the DSS colitis model, the EcN WT was recovered in higher numbers from the cecum and colon than the Δ*fdnG fdoG* mutant (~4-fold; Fig. 4A and S5C). The phenotype of the Δ*fdnG fdoG* mutant was fully recapitulated by a mutant lacking only FDN (Δ*fdnG* mutant), while FDO activity was dispensable. To exclude the possibility that formate utilization is a unique property of EcN, we analyzed the lab-adapted *E. coli* strain K-12 as well as the Adherent Invasive *E. coli* strain (AIEC) NRG857c (Eaves-Pyles et al., 2008) originally isolated from an IBD patient (Fig. 4A, S5C and S5D). No strain-specific effects on the induction of mucosal inflammation were noted as determined by the pro-inflammatory marker *Tnfa* (Fig. 4B), a major mediator of disease in IBD patients (Baumgart and Sandborn, 2012). Akin to the findings with EcN, formate dehydrogenases, in particular FDN, enhanced fitness of these human *E. coli* strains in the DSS colitis model (Fig. 4A and S5C).

Next, we analyzed formate utilization in the murine commensal SL1 in the colon and cecum lumen (Fig. 4C, S1C, and S6A-C). In the absence of inflammation, colonization of the large intestine by SL1 was moderate (Fig. S6A) and formate dehydrogenase activity conferred a minimal competitive growth advantage (Fig. 4C, S6A and B). In contrast, SL1 colonized the colon in large numbers in the DSS colitis model (Fig. S6A) and the SL1 WT outcompeted the formate dehydrogenase-deficient mutant (8-fold in the colon content; Fig. 4C and S6A). This effect was independent of the inoculum size (Fig. S7A).

DSS-induced colitis is a model of epithelial injury. To determine whether *E. coli* relies on formate oxidation in other models of colitis, we performed competitive colonization experiments in a genetic model of colitis. Mice deficient for the anti-inflammatory cytokine IL-10 (encoded by *Il10*) spontaneously develop colitis, a process that can be accelerated by oral administration of piroxicam (Berg et al., 2002). Piroxicam-treated, *Il10*-deficient C57BL/6 mice were intragastrically inoculated with an equal mixture of the SL1 WT and the Δ*fdnG* Δ*fdoG* mutant. After one week, markers of inflammation were markedly elevated (Fig. S6C) and the SL1 WT outcompeted the formate dehydrogenase-deficient mutant (Fig. 4C and S6B). Similar results were obtained using piroxicam-treated, *Il10*-deficient BALB/c mice (Fig. 4C, S6B and C). Furthermore, the AIEC NRG857c WT outcompeted the formate oxidation-deficient mutant in piroxicam-treated, *Il10*-deficient C57BL/6 mice (Fig. S6D and E). We also analyzed a T cell transfer model of colitis (Fig. S1D). After development of intestinal inflammation, animals were colonized with an equal mixture of the murine commensal *E. coli* SL1 WT and an isogenic Δ*fdnG* Δ*fdoG* mutant. After nine days, *Nos2*

and *Tnfa* mRNA levels were significantly increased compared to control C57BL/6 animals (Fig. S6C). Most importantly, the WT outcompeted the formate oxidation-deficient mutant (Fig. 4C and S6B). Collectively, these experiments demonstrate that formate dehydrogenases provide a fitness advantage to *E. coli* in the inflamed gut.

Formate oxidation contributes to the expansion of *E. coli* during inflammation-associated dysbiosis

While the design of the previous experiments (inoculation with indicator strains after onset of colitis) allowed us to study the role of metabolic pathways in an inflammatory environment, we next sought a more relevant experimental setting in which animals are colonized with *E. coli* indicator strains prior to the induction of inflammation. Animals, intragastrically inoculated with an equal mixture of the EcN WT and the Δ*fdnG fdoG* mutant, received DSS in the drinking water for 8 days followed by one day of normal drinking water to remove DSS contamination from tissue samples (Fig. S1C). The EcN WT was recovered at significantly higher numbers than the formate dehydrogenase-deficient mutant from the colon (competitive index of 55-fold) and cecum (51-fold) (Fig. 5A). To test whether formate oxidation would also enhance fitness of *E. coli* in competition with the native microbiota, we intragastrically inoculated two groups of mice with the EcN WT and the Δ*fdnG fdoG* mutant, respectively (Fig. 5B-E and S7B). Inflammation was induced to a similar extent in both groups (Fig. 5B-D). The WT colonized the colon and cecum lumen at high numbers, while the Δ*fdnG fdoG* mutant was defective for efficient colonization of the intestinal lumen (Fig. 5E and S7B), indicating that formate oxidation contributes to fitness of *E. coli* during episodes of inflammation.

Formate in the gut lumen is microbiota-derived

Formate is a common microbial fermentation end product (Patel et al., 2014; Ragsdale, 2003; Sawers and Clark, 2004). To test whether formate is indeed derived from the gut microbiota, we performed a competition experiment with the EcN WT and the formate dehydrogenase-deficient mutant in DSS-treated, gnotobiotic Swiss-Webster mice. DSS treatment induced mucosal inflammation to a similar extent as in conventional C57BL/6 mice (Fig. 4B, 5D, 6A, S6C). Consistent with the idea that the microbiota is a major producer of formate, the ability to utilize formate was dispensable for *E. coli* to colonize the colon of DSS-treated (ex-)germ-free mice (Fig. 6B and S7C).

Conversion of pyruvate to acetyl-CoA by pyruvate formate lyase liberates formate. Pyruvate formate lyase is expressed by a wide range of microorganisms, including *Bacteroides* species. Mono-association of germ-free mice with *B. thetaiotaomicron*, a prototypical *Bacteroides* species, was sufficient to restore formate oxidation in *E. coli* (Fig. 6B S1E, and S7C). Similarly, transfer of the intestinal microbiota from conventionally-raised mice to germ-free Swiss-Webster mice restored the phenotype of the Δ*fdnG fdoG* mutant (Fig. 6B and S7C). Taken together, these experiments indicate that formate is present during episodes of inflammation is derived from the gut microbiota.

Concentration of formate is increased during inflammation

To determine the concentration of extracellular formate in the gut lumen, we measured formate concentrations in the colon content of mock-treated and DSS-treated mice by GC/MS 7 days after the start of the DSS treatment (Fig. 6C, 6D, S7D and E). The concentration of formate in the extracellular environment of the gut lumen was increased significantly during DSS treatment compared to mock-treated mice (Fig. 6D). As a control, we determined that the extraction method did not result in the lysis of commensal bacteria (Fig. S7D). Formate levels were significantly lower in mock-or DSS-treated germ-free mice compared to conventionally reared animals (Fig. 6D), indicating that the majority of formate is of microbial origin.

Terminal oxidase activity is required for formate oxidation *in vivo*

Due to its oxidation to CO_2, formate is a poor carbon source for Enterobacteriaceae (Gutnick et al., 1969), as it would require subsequent carbon fixation of CO_2. Therefore, the physiological importance of formate oxidation in Enterobacteriaceae likely results from the use of formate as an electron donor for the electron transport chain. This raises the question as to what electron acceptor is used for formate oxidation *in vivo*. In principle, *E. coli* can utilize several terminal electron acceptors, including oxygen, nitrate, *S*-oxides, *N*-oxides, nitrite, and fumarate *in vitro* (Unden et al., 2014). Our data indicate that nitrate respiration occurs in the inflamed gut (Winter et al., 2013b)(Fig. 3A). We thus asked whether formate oxidation could provide a fitness advantage in the absence of nitrate respiration and performed a competitive colonization experiment in the DSS colitis model with a nitrate reductase-deficient strain (NR mutant) and a mutant lacking both nitrate reductase and formate dehydrogenase activity (NR Δ*fdnG fdoG* mutant) (Fig. 7A and S7F). The phenotype of formate oxidation was recapitulated in the absence of nitrate reductase activity, suggesting that nitrate is unlikely to be the electron acceptor for formate *in vivo*. *S*-oxides, *N*-oxides and nitrite reduction did not appear to enhance colonization (Fig. 3A) and were not further investigated. The *E. coli* genome is predicted to encode three terminal oxidases for oxygen respiration. The cytochrome bo_3 ubiquinol oxidase CyoABCDE is only active during highly oxygenated conditions while the *cyxAB* genes, predicted to encode a cytochrome bd oxidase, are cryptic. We therefore focused our attention on the cytochrome bd oxidase CydAB, which is expressed under microaerobic conditions. We generated a mutant lacking the major subunit (Δ*cydA* mutant) as well as a mutant lacking both CydAB and formate dehydrogenase activity (Δ*cydA* Δ*fdnG fdoG* mutant). In the DSS colitis model, both strains were recovered at an equal ratio (Fig. 7A and S7F), suggesting that terminal oxidase activity is required for formate oxidation *in vivo*. Mirroring these findings, formate oxidation provided a fitness advantage under microaerobic conditions *in vitro* (Fig. S5A). In the absence of CydAB, the fitness advantage conferred by formate oxidation was negated compared to the competition experiment with the WT and the *fdoG fdnG* mutant. This result suggested that aerobic respiration is required for formate oxidation under microaerobic conditions *in vitro*. Curiously, nitrate was required for enabling formate oxidation under microaerobic conditions. Nitrate induces FDN expression in *E. coli* K-12 (Abaibou et al., 1995; Berg and Stewart, 1990; Wang and Gunsalus, 2003) and EcN *in vitro* (Fig. S5E). Thus, nitrate stimulates full formate dehydrogenase activity under microaerobic conditions.

The respiratory cytochrome bd oxidase CydAB is required for colonization during DSS-induced colitis

The finding that formate dehydrogenases are linked to oxygen respiration raises the possibility that changes in oxygen availability may play a role in shaping gut microbial communities during inflammation. Consistent with this notion, our metagenomics analysis had revealed an additional signature of microbial dysbiosis, i.e. oxygen respiration through terminal oxidases (Fig. 1C and S2). Mapping of metagenomics sequence reads to representative terminal oxidase operons confirmed that genes encoding terminal oxidases were indeed enriched in the microbiome of DSS-treated animals (Fig. 7B).

To investigate whether oxygen respiration would indeed confer a fitness advantage to facultative anaerobic bacteria, we determined the contribution of terminal oxidases to fitness of *E. coli* in the DSS colitis model through a competition experiment. In the absence of inflammation, the EcN WT and the *cydAB* mutant colonized the cecum and colon content at low, but comparable levels (Fig. 7C and D). When inflammation was induced (DSS), the EcN WT was recovered at high numbers while the Δ*cydAB* mutant colonized poorly, suggesting that the cytochrome bd-oxidase CydAB is required for the expansion of the *E. coli* population during DSS-induced inflammation. The CyoABCDE enzyme was not required as the Δ*cyoABCDE* mutant colonized the cecum and colon content at levels comparable to the WT.

DISCUSSION

Intestinal inflammation is associated with gut microbiota dysbiosis that favors an expansion of the Enterobacteriaceae population, however the mechanisms underlying these phylum-level changes remain poorly characterized. Here, we performed a metagenomic analysis to identify microbial genes that are enriched in cecal microbial communities during inflammation and to discover pathways that contribute to bacterial dysbiosis. Our results identify MoCo-dependent enzymes as well as components of the aerobic respiratory chain as signatures of inflammation-associated dysbiosis in the murine cecum. The murine cecum and colon are distinct sites with different microbial ecologies. To validate our findings from the metagenomic sequencing analysis, we determined the contribution of select metabolic pathways, i.e. formate oxidation and oxygen respiration, to colonization of the cecum and colon using bacterial model organisms. Inactivation of MoCo biosynthesis in members of the Enterobacteriaceae family such as *E. coli, K. oxytoca*, and *E. cloacae* resulted in decreased fitness in the inflamed gut (Fig. 2), suggesting that MoCo-dependent enzymes are required for the bloom of the Enterobacteriaceae population during bouts of inflammation.

Previous work had established a mechanism by which bacterial nitrate respiration, a MoCo-dependent process, enhances luminal growth of *E. coli* in animal models of colitis (Winter et al., 2013b). Our metagenomic analysis also suggested that in addition to nitrate reduction, other MoCo-dependent enzymes such as formate dehydrogenases, are associated with bacterial dysbiosis and might facilitate changes in the composition of the microbiota. By focusing on commensal *E. coli* strains, we found that formate oxidation by the FDN enzyme enhances fitness and colonization of the intestinal lumen. The ability to utilize formate is widespread between Enterobacteriaceae family members, but other bacterial phyla express

formate dehydrogenases. For example, members of the phylum Verrucomicrobia are predicted to encode formate dehydrogenases (Hou et al., 2008), which may explain the occasional expansion of this population during colitis (Fig. 1A) (Nagalingam et al., 2011). Methanogenic archaea found in the human colon have been shown to utilize formate during normal gut colonization (Samuel and Gordon, 2006). The ability to utilize formate is necessary for *E. coli* to colonize the inflamed gut since mutants lacking formate dehydrogenase genes are defective for efficient gut colonization (Fig. 4). These considerations suggest that formate oxidation contributes to the inflammation-associated bloom of Enterobacteriaceae, however, it is not a sufficient property since not all microorganisms capable of utilizing formate bloom during inflammation. Also, the Enterobacteriaceae population in our DSS colitis model expands by about 6 orders of magnitude, while the contribution of MoCo-dependent processes is about 2 orders of magnitude (Fig. 2B and C). In addition to nitrate respiration and formate oxidation other unknown factors likely contribute to the inflammation-associated bloom of Enterobacteriaceae.

In Enterobacteriaceae, FDN and FDO enable the use of formate as an electron donor for the electron transport chain (Sawers et al., 2004). Curiously, our experiments suggest that oxygen is the electron acceptor for formate oxidation (Fig. 7A) and the high-affinity cytochrome bd-oxidase CydAB is required for colonization during DSS-induced colitis. These results suggest that oxygen enters the otherwise anaerobic gut lumen during episodes of inflammation. Previous studies have revealed that the metabolism of mature colonocytes has a significant impact on the availability of molecular oxygen at the gut mucosal surface. Under homeostatic conditions, mature colonocytes utilize microbiota-derived butyrate as the primary carbon source through β-oxidation, thus depleting oxygen levels at the mucosal interface and generating an anaerobic environment in the gut lumen (Kelly et al., 2015; Rivera-Chavez et al., 2016). Induction of inflammation, either by administration of DSS or infection with an enteric pathogen, impairs the ability of the large intestinal epithelium to perform β-oxidation (Ahmed et al., 2012; Kelly et al., 2015; Lopez et al., 2016; Rivera-Chavez et al., 2016). Consequently, oxygen is predicted to diffuse in the gut lumen. Increased availability of oxygen in the gut lumen has been reported to promote colonization with facultative anaerobic enteric pathogens (Lopez et al., 2016; Rivera-Chavez et al., 2016). Thus, it is plausible that the oxygen tension in the gut lumen rises during non-infectious colitis, an idea termed “oxygen hypothesis” (Rigottier-Gois, 2013). Our data in the DSS colitis model provide experimental support for this hypothesis since formate oxidation by *E. coli* requires respiration and respiratory genes are required for efficient gut colonization (Fig. 7). Furthermore, genes encoding terminal oxidases were enriched in microbial communities in the DSS colitis model (Fig. 1).

The ability to break down pyruvate to formate and acetyl-CoA is highly conserved and present in virtually all major phylogenetic groups of the gut microbiota, including *Bacteroides* and *Clostridia* (Lehtio and Goldman, 2004; Thauer et al., 1972). In our experiments, induction of inflammation by DSS resulted in a moderate increase in luminal formate levels (Fig. 6C). Since formate is available during homeostasis, it is possible that the increased availability of oxygen may enable *E. coli* to access the formate pool and utilize this energetically valuable electron donor during inflammation.

FDN is thought to form a respiratory module with nitrate respiration *in vitro* while the electron acceptor for formate dehydrogenase-O is thought to be oxygen. This effect is likely due to gene regulation since FDO is expressed constitutively at low levels and FDN expression is induced by exogenous formate and nitrate (Abaibou et al., 1995; Berg and Stewart, 1990; Wang and Gunsalus, 2003)(Fig. S5E). Our results from the DSS colitis model indicate that *E. coli* predominantly relies on the FDN enzyme with oxygen likely serving as the terminal electron acceptor. It is tempting to speculate that inflammation-derived nitrate (Winter et al., 2013b) induces the expression of FDN, thus making the FDN enzyme the predominant formate dehydrogenase in this environment. Consistent with this idea, addition of nitrate to the culture media enhanced oxygen-dependent formate oxidation under microaerobic conditions *in vitro* (Fig. S5A).

We conclude that formate oxidation and oxygen respiration represent metabolic signatures of gut microbiota dysbiosis. Furthermore, formate oxidation, in conjunction with respiration, constitutes a mechanism for Enterobacteriaceae outgrowth during inflammation-associated dysbiosis.

EXPERIMENTAL PROCEDURES

Bacterial strains

The bacterial strains used in this study, strain construction procedures, growth medium details, and methods of isolation of commensal Enterobacteriaceae are listed in Supplemental Experimental Procedures.

Mouse experiments

Male and female 6-12 week old wild-type (WT) C57BL/6, WT Swiss Webster, *Il10* knockout (KO) C57BL/6, *Il10* KO BALB/c and *Rag1* KO C57BL/6 mice were used. Mice were specific pathogen free or germ-free. Colitis was induced with 2 % or 3 % dextran sulfate sodium (DSS; Alfa Aesar) (Winter et al., 2013b). *Il10* KO mice were fed Piroxicam chow (50 ppm or 100 ppm; Teklad custom research diets, Envigo). Mice which were not colonized were excluded from analysis. *Rag1* KO mice were injected intraperitoneally with naïve T cells from spleens of C57BL/6 mice. At the indicated time points, mice received the indicated strains by intragastric gavage.

Metagenomics

Genomic DNA from cecal content was isolated using the PowerFecal DNA Isolation kit (MoBio). A blastX database was created in DIAMOND (Buchfink et al., 2015). Taxonomic comparisons were performed in MEtaGenome ANalyzer version 5 (Huson et al., 2007). Metabolic pathway analysis was performed by comparing the blastx results to the KEGG and SEED databases. To map reads to bacterial metabolic genes, the Enterobacteriaceae operons of interest were downloaded from KEGG and reads mapped to gene clusters using the BBmap tool.

Histopathology

Fomalin-fixed tissue was embedded in paraffin and stained with hematoxylin and eosin. The samples were blinded and scored as described in Supplemental table 4.

Quantitative real-time PCR

RNA was extracted via the TRI reagent method (Molecular Research Center), mRNA purified with NEBNext Poly(A) mRNA Magnetic Isolation Module (New England Biolabs), and then cDNA synthesized with TaqMan reverse transcription reagents (Life Technologies). qPCR was performed in a QuantStudio 6 Flex Instrument (Life Technologies) with SYBR Green (Life Technologies), using primers listed in Supplemental Table 4.

Measurement of formate concentrations

Colon content was supplemented with deuterated sodium formate (Sigma-Aldrich). Sodium formate (Sigma-Aldrich) supplemented with deuterated sodium formate was used for standards. Ethyl acetate extracts of formic acid were derivatized prior to GC-MS analysis (Shimadzu, TQ8040)).

In vitro experiments

Competition assays were performed with *E. coli* (1×10^3 CFU/mL starting concentration) in mucin broth with exogenous compounds under microaerobic, aerobic or anaerobic conditions for 18 h or 16 h at 37 °C. Growth curves were performed aerobically or anaerobically at 37 #x000B0;C in M9 medium, with a starting concentration of 1×10^8 CFU/mL *E. coli*. For the nitrate reductase assays, bacterial cultures supplemented with sodium nitrate were incubated at 37 °C 2 hours before reading the OD_{600}. Marshall's reagent was incubated with the cultures for 10 minutes. OD_{420} and OD_{540} were measured (BioTek) and nitrate reductase activities calculated: NR Activity = $(OD_{540} - 0.72\times OD_{420})/(0.06\times120\times OD_{600})$.

Statistical analysis

Differences between groups were analyzed by unpaired Student's *t*-test, unless stated otherwise. *P* values of less than 0.05 were considered statistically significant. Fold changes in mRNA levels, bacterial loads, competitive indices, and formate concentrations underwent natural logarithmic transformations prior to statistical analysis.

Ethics statement

All mouse experiments were reviewed and approved by the Institutional Animal Care and Use Committee at UT Southwestern Medical Center (APN# 2013-0159, 2016-101681, and 2015-0031).

Supplementary Material

Refer to Web version on PubMed Central for supplementary material.

Acknowledgments

This work was funded by Public Health Service Grants AI118807 (S.E.W.), DK102436 (B.A.D.), AI007520 (E.R.H), GM109776 (E.R.H., C.G.), The Welch Foundation (I-1858; S.E.W.). C.G. was supported by a NSF Graduate Research Fellowship (1000194723). The funders had no role in study design, data collection and interpretation, or the decision to submit the work for publication. Any opinions, findings, and conclusions or recommendations expressed in this material are those of the author(s) and do not necessarily reflect the views of the NSF or NIH. We thank Dr. A. Torres for kindly providing NRG 857C, Everton de Lima Romao for technical assistance, and Drs. R. Tsolis, V. Sperandio, J. Pfeiffer, and D. Hendrixson for helpful discussion.

REFERENCES

Abaibou H, Pommier J, Benoit S, Giordano G, Mandrand-Berthelot MA. Expression and characterization of the Escherichia coli fdo locus and a possible physiological role for aerobic formate dehydrogenase. J Bacteriol. 1995; 177:7141–7149. [PubMed: 8522521]

Ahmed I, Chandrakesan P, Tawfik O, Xia L, Anant S, Umar S. Critical roles of Notch and Wnt/beta-catenin pathways in the regulation of hyperplasia and/or colitis in response to bacterial infection. Infect Immun. 2012; 80:3107–3121. [PubMed: 22710872]

Baumgart DC, Sandborn WJ. Crohn's disease. Lancet. 2012; 380:1590–1605. [PubMed: 22914295]

Baumgart M, Dogan B, Rishniw M, Weitzman G, Bosworth B, Yantiss R, Orsi RH, Wiedmann M, McDonough P, Kim SG, et al. Culture independent analysis of ileal mucosa reveals a selective increase in invasive Escherichia coli of novel phylogeny relative to depletion of Clostridiales in Crohn's disease involving the ileum. ISME J. 2007; 1:403–418. [PubMed: 18043660]

Berg BL, Stewart V. Structural genes for nitrate-inducible formate dehydrogenase in Escherichia coli K-12. Genetics. 1990; 125:691–702. [PubMed: 2168848]

Berg DJ, Zhang J, Weinstock JV, Ismail HF, Earle KA, Alila H, Pamukcu R, Moore S, Lynch RG. Rapid development of colitis in NSAID-treated IL-10-deficient mice. Gastroenterology. 2002; 123:1527–1542. [PubMed: 12404228]

Berry D, Schwab C, Milinovich G, Reichert J, Ben Mahfoudh K, Decker T, Engel M, Hai B, Hainzl E, Heider S, et al. Phylotype-level 16S rRNA analysis reveals new bacterial indicators of health state in acute murine colitis. ISME J. 2012; 6:2091–2106. [PubMed: 22572638]

Blattner FR, Plunkett G 3rd, Bloch CA, Perna NT, Burland V, Riley M, Collado-Vides J, Glasner JD, Rode CK, Mayhew GF, et al. The complete genome sequence of Escherichia coli K-12. Science. 1997; 277:1453–1462. [PubMed: 9278503]

Buchfink B, Xie C, Huson DH. Fast and sensitive protein alignment using DIAMOND. Nat Methods. 2015; 12:59–60. [PubMed: 25402007]

Cheng VW, Weiner JH. S- and N-Oxide Reductases. EcoSal Plus. 2007; 2

Cockburn DW, Koropatkin NM. Polysaccharide Degradation by the Intestinal Microbiota and Its Influence on Human Health and Disease. J Mol Biol. 2016

Cole JA, Richardson DJ. Respiration of Nitrate and Nitrite. EcoSal Plus. 2008; 3

Eaves-Pyles T, Allen CA, Taormina J, Swidsinski A, Tutt CB, Jezek GE, Islas-Islas M, Torres AG. Escherichia coli isolated from a Crohn's disease patient adheres, invades, and induces inflammatory responses in polarized intestinal epithelial cells. Int J Med Microbiol. 2008; 298:397–409. [PubMed: 17900983]

Eilam O, Zarecki R, Oberhardt M, Ursell LK, Kupiec M, Knight R, Gophna U, Ruppin E. Glycan degradation (GlyDeR) analysis predicts mammalian gut microbiota abundance and host diet-specific adaptations. MBio. 2014; 5

Faith JJ, McNulty NP, Rey FE, Gordon JI. Predicting a human gut microbiota's response to diet in gnotobiotic mice. Science. 2011; 333:101–104. [PubMed: 21596954]

Fischbach MA, Sonnenburg JL. Eating for two: how metabolism establishes interspecies interactions in the gut. Cell host & microbe. 2011; 10:336–347. [PubMed: 22018234]

Flint HJ, Scott KP, Duncan SH, Louis P, Forano E. Microbial degradation of complex carbohydrates in the gut. Gut Microbes. 2012; 3:289–306. [PubMed: 22572875]

Frank DN, St Amand AL, Feldman RA, Boedeker EC, Harpaz N, Pace NR. Molecular-phylogenetic characterization of microbial community imbalances in human inflammatory bowel diseases. Proc Natl Acad Sci U S A. 2007; 104:13780–13785. [PubMed: 17699621]

Giaffer MH, Holdsworth CD, Duerden BI. The assessment of faecal flora in patients with inflammatory bowel disease by a simplified bacteriological technique. J Med Microbiol. 1991; 35:238–243. [PubMed: 1941994]

Gutnick D, Calvo JM, Klopotowski T, Ames BN. Compounds which serve as the sole source of carbon or nitrogen for Salmonella typhimurium LT-2. J Bacteriol. 1969; 100:215–219. [PubMed: 4898986]

Hou S, Makarova KS, Saw JH, Senin P, Ly BV, Zhou Z, Ren Y, Wang J, Galperin MY, Omelchenko MV, et al. Complete genome sequence of the extremely acidophilic methanotroph isolate V4, Methylacidiphilum infernorum, a representative of the bacterial phylum Verrucomicrobia. Biol Direct. 2008; 3:26. [PubMed: 18593465]

Huson DH, Auch AF, Qi J, Schuster SC. MEGAN analysis of metagenomic data. Genome Res. 2007; 17:377–386. [PubMed: 17255551]

Kelly CJ, Zheng L, Campbell EL, Saeedi B, Scholz CC, Bayless AJ, Wilson KE, Glover LE, Kominsky DJ, Magnuson A, et al. Crosstalk between Microbiota-Derived Short-Chain Fatty Acids and Intestinal Epithelial HIF Augments Tissue Barrier Function. Cell host & microbe. 2015; 17:662–671. [PubMed: 25865369]

Koropatkin NM, Cameron EA, Martens EC. How glycan metabolism shapes the human gut microbiota. Nat Rev Microbiol. 2012; 10:323–335. [PubMed: 22491358]

Lehtio L, Goldman A. The pyruvate formate lyase family: sequences, structures and activation. Protein Eng Des Sel. 2004; 17:545–552. [PubMed: 15292518]

Leimkuhler S, Iobbi-Nivol C. Bacterial molybdoenzymes: old enzymes for new purposes. FEMS Microbiol Rev. 2016; 40:1–18. [PubMed: 26468212]

Lopez CA, Miller BM, Rivera-Chavez F, Velazquez EM, Byndloss MX, Chavez-Arroyo A, Lokken KL, Tsolis RM, Winter SE, Baumler AJ. Virulence factors enhance Citrobacter rodentium expansion through aerobic respiration. Science. 2016; 353:1249–1253. [PubMed: 27634526]

Lupp C, Robertson ML, Wickham ME, Sekirov I, Champion OL, Gaynor EC, Finlay BB. Host-mediated inflammation disrupts the intestinal microbiota and promotes the overgrowth of Enterobacteriaceae. Cell host & microbe. 2007; 2:119–129. [PubMed: 18005726]

Magalon A, Mendel RR. Biosynthesis and Insertion of the Molybdenum Cofactor. EcoSal Plus. 2008; 3

Martens EC, Kelly AG, Tauzin AS, Brumer H. The devil lies in the details: how variations in polysaccharide fine-structure impact the physiology and evolution of gut microbes. J Mol Biol. 2014; 426:3851–3865. [PubMed: 25026064]

Nagalingam NA, Kao JY, Young VB. Microbial ecology of the murine gut associated with the development of dextran sodium sulfate-induced colitis. Inflamm Bowel Dis. 2011; 17:917–926. [PubMed: 21391286]

Patel MS, Nemeria NS, Furey W, Jordan F. The pyruvate dehydrogenase complexes: structure-based function and regulation. J Biol Chem. 2014; 289:16615–16623. [PubMed: 24798336]

Raetz M, Hwang SH, Wilhelm CL, Kirkland D, Benson A, Sturge CR, Mirpuri J, Vaishnava S, Hou B, Defranco AL, et al. Parasite-induced TH1 cells and intestinal dysbiosis cooperate in IFN-gamma-dependent elimination of Paneth cells. Nat Immunol. 2013; 14:136–142. [PubMed: 23263554]

Ragsdale SW. Pyruvate ferredoxin oxidoreductase and its radical intermediate. Chem Rev. 2003; 103:2333–2346. [PubMed: 12797832]

Rigottier-Gois L. Dysbiosis in inflammatory bowel diseases: the oxygen hypothesis. ISME J. 2013; 7:1256–1261. [PubMed: 23677008]

Rivera-Chavez F, Zhang LF, Faber F, Lopez CA, Byndloss MX, Olsan EE, Xu G, Velazquez EM, Lebrilla CB, Winter SE, et al. Depletion of Butyrate-Producing Clostridia from the Gut Microbiota Drives an Aerobic Luminal Expansion of Salmonella. Cell host & microbe. 2016; 19:443–454. [PubMed: 27078066]

Ruiz-Herrera J, Showe MK, DeMoss JA. Nitrate reductase complex of Escherichia coli K-12: isolation and characterization of mutants unable to reduce nitrate. Journal of bacteriology. 1969; 97:1291–1297. [PubMed: 4887509]

Samuel BS, Gordon JI. A humanized gnotobiotic mouse model of host-archaeal-bacterial mutualism. Proc Natl Acad Sci U S A. 2006; 103:10011–10016. [PubMed: 16782812]

Sawers RG, Blokesch M, Bock A. Anaerobic Formate and Hydrogen Metabolism. EcoSal Plus. 2004; 1

Sawers RG, Clark DP. Fermentative Pyruvate and Acetyl-Coenzyme A Metabolism. EcoSal Plus. 2004:1.

Scott RH, DeMoss JA. Formation of the formate-nitrate electron transport pathway from inactive components in Escherichia coli. Journal of bacteriology. 1976; 126:478–486. [PubMed: 770433]

Seksik P, Rigottier-Gois L, Gramet G, Sutren M, Pochart P, Marteau P, Jian R, Dore J. Alterations of the dominant faecal bacterial groups in patients with Crohn's disease of the colon. Gut. 2003; 52:237–242. [PubMed: 12524406]

Shin NR, Whon TW, Bae JW. Proteobacteria: microbial signature of dysbiosis in gut microbiota. Trends Biotechnol. 2015; 33:496–503. [PubMed: 26210164]

Sonnenburg ED, Zheng H, Joglekar P, Higginbottom SK, Firbank SJ, Bolam DN, Sonnenburg JL. Specificity of polysaccharide use in intestinal bacteroides species determines diet-induced microbiota alterations. Cell. 2010; 141:1241–1252. [PubMed: 20603004]

Sonnenburg JL, Backhed F. Diet-microbiota interactions as moderators of human metabolism. Nature. 2016; 535:56–64. [PubMed: 27383980]

Stecher B, Robbiani R, Walker AW, Westendorf AM, Barthel M, Kremer M, Chaffron S, Macpherson AJ, Buer J, Parkhill J, et al. Salmonella enterica serovar typhimurium exploits inflammation to compete with the intestinal microbiota. PLoS biology. 2007; 5:2177–2189. [PubMed: 17760501]

Tasman A, Pot AW. The formation of hydrogen from glucose and formic acid by the so-called "resting" B. coli. I. The Biochemical journal. 1935; 29:1749–1756. [PubMed: 16745842]

Thauer RK, Kirchniawy FH, Jungermann KA. Properties and function of the pyruvate-formate-lyase reaction in clostridiae. Eur J Biochem. 1972; 27:282–290. [PubMed: 4340563]

Unden G, Steinmetz PA, Degreif-Dunnwald P. The Aerobic and Anaerobic Respiratory Chain of Escherichia coli and Salmonella enterica: Enzymes and Energetics. EcoSal Plus. 2014

Vujkovic-Cvijin I, Dunham RM, Iwai S, Maher MC, Albright RG, Broadhurst MJ, Hernandez RD, Lederman MM, Huang Y, Somsouk M, et al. Dysbiosis of the gut microbiota is associated with HIV disease progression and tryptophan catabolism. Sci Transl Med. 2013; 5:193ra191.

Wang H, Gunsalus RP. Coordinate regulation of the Escherichia coli formate dehydrogenase fdnGHI and fdhF genes in response to nitrate, nitrite, and formate: roles for NarL and NarP. J Bacteriol. 2003; 185:5076–5085. [PubMed: 12923080]

Winter SE, Lopez CA, Baumler AJ. The dynamics of gut-associated microbial communities during inflammation. EMBO reports. 2013a; 14:319–327. [PubMed: 23478337]

Winter SE, Winter MG, Xavier MN, Thiennimitr P, Poon V, Keestra AM, Laughlin RC, Gomez G, Wu J, Lawhon SD, et al. Host-derived nitrate boosts growth of E. coli in the inflamed gut. Science. 2013b; 339:708–711. [PubMed: 23393266]

Wrigley CW, Linnane AW. Formic acid dehydrogenasecytochrome b1 complex from Escherichia coli. Biochemical and biophysical research communications. 1961; 4:66–70. [PubMed: 13786837]

Wu GD, Chen J, Hoffmann C, Bittinger K, Chen YY, Keilbaugh SA, Bewtra M, Knights D, Walters WA, Knight R, et al. Linking long-term dietary patterns with gut microbial enterotypes. Science. 2011; 334:105–108. [PubMed: 21885731]

HIGHLIGHTS

- Genes encoding respiratory pathways are overrepresented in the dysbiotic microbiome
- Utilization of microbiota-derived formate enhances *E. coli* fitness in the inflamed gut
- Formate concentrations in the gut are elevated during inflammation-associated dysbiosis
- During gut inflammation, formate utilization by *E. coli* requires oxygen respiration

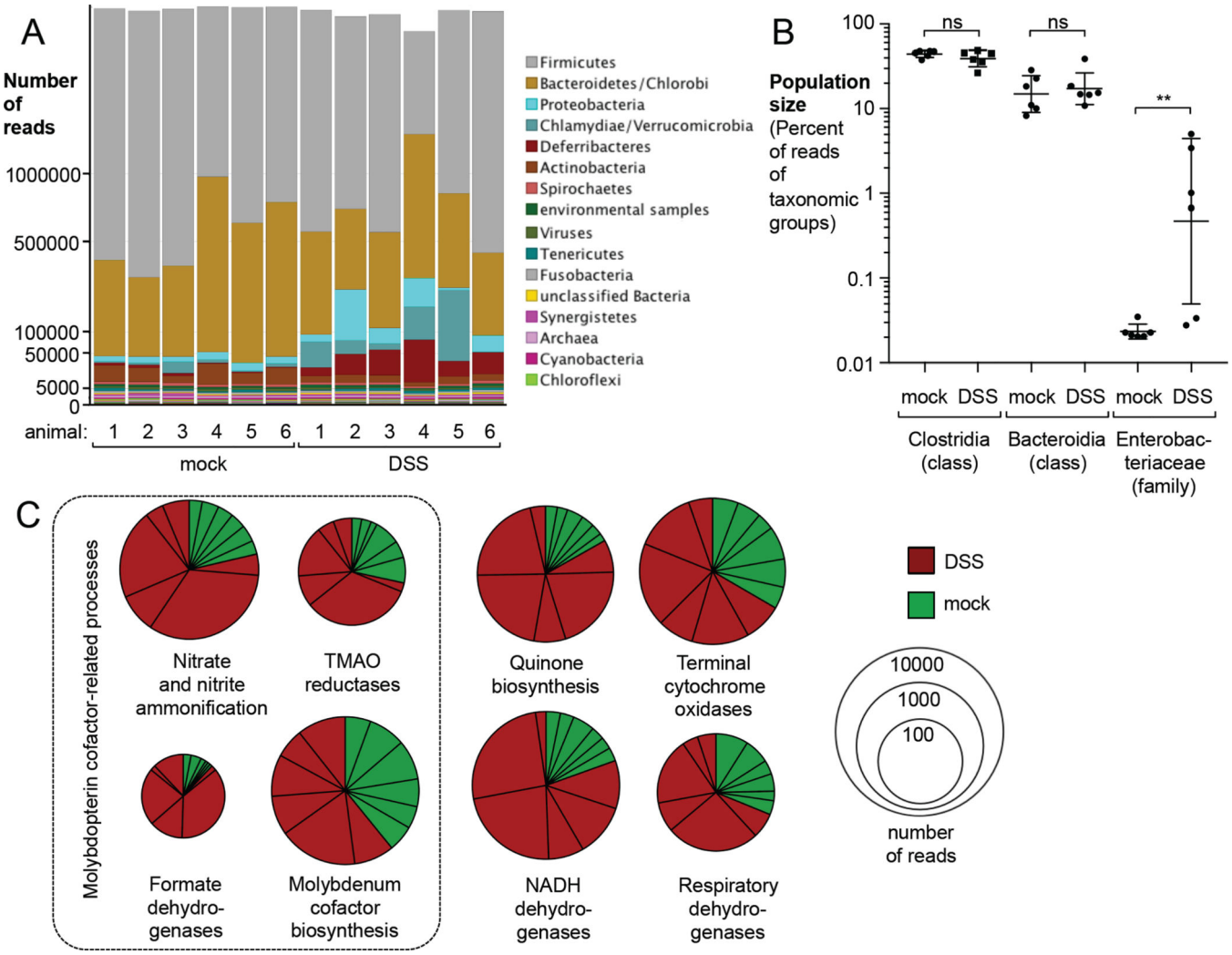

Figure 1. Intestinal inflammation induces changes in the cecal microbiome

Groups of specific pathogen free (SPF) mice (N = 6 per group) were treated with 3 % dextran sulfate sodium (DSS) in the drinking water for 9 days or mock-treated. DNA, extracted from cecal content, was subjected to shotgun metagenomic sequencing. (A) Phylogenetic composition of the gut microbiota at the phylum level. (B) Percent of total reads corresponding to the taxonomic groups Clostridia (class), Bacteroidia (class), and Enterobacteriaceae (family). Each dot represents one animal. Lines represent the geometric mean ± standard deviation. ns, not statistically significant; **, $P < 0.01$ (C) Enrichment of pathways related to molybdopterin-cofactor biosynthesis and the electron transport chain in DSS-treated (red) compared to mock-treated mice (green). The size of the circle chart is proportional to the combined number of reads for all animals. Each slice represents one animal with the arc length being a measure of the number of reads from each mouse (see also Figure S2).

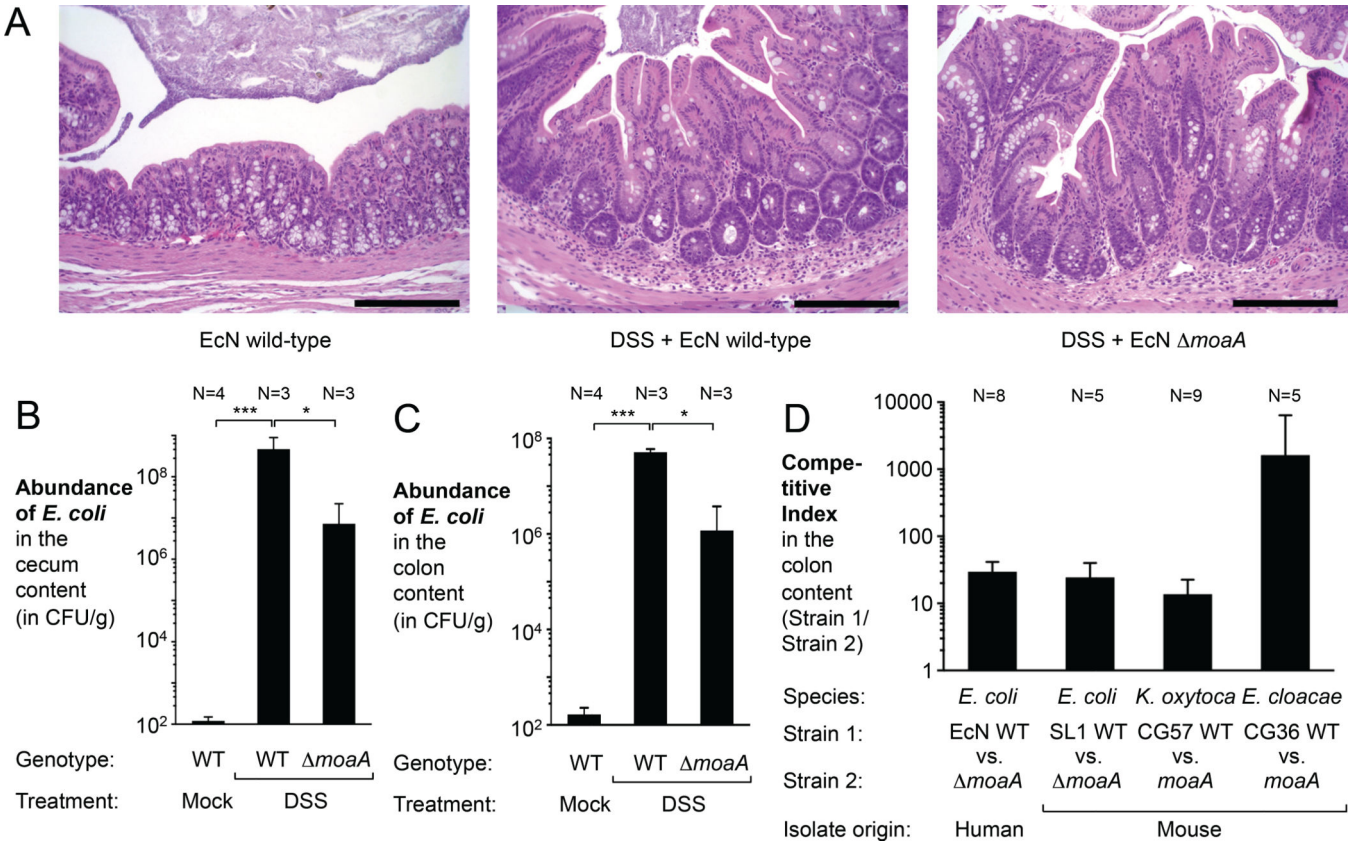

Figure 2. Molybdopterin cofactor contributes to fitness of Enterobacteriaceae in the DSS-induced colitis model

(A-C) Groups of SPF C57BL/6 mice were treated with 3 % DSS or water (mock). After four days, animals were intragastrically inoculated with the *E. coli* Nissle 1917 (EcN) wild-type strain (WT) or an isogenic Δ*moaA* mutant. Samples were analyzed five days after inoculation (see also Figure S3A – E). (A) Representative images of hematoxylin and eosin-stained cecal sections. Scale bar, 200 μm. (B and C) Abundances of the experimentally introduced *E. coli* strains in the cecum (B) and colon (C) content. (D) Groups of SPF C57BL/6 mice, treated with 3 % DSS for 4 days, were intragastrically inoculated with an equal mixture of the indicated wild-type (WT) Enterobacteriaceae strains and isogenic *moaA* mutants and DSS treatment was continued. Five days after inoculation, the abundance of each strain was determined and the ratio (competitive index) of the two strains calculated. Bars represent geometric means ± standard error. The number of mice per group (N) is indicated in each panel. *, $P < 0.05$; ***, $P < 0.001$.

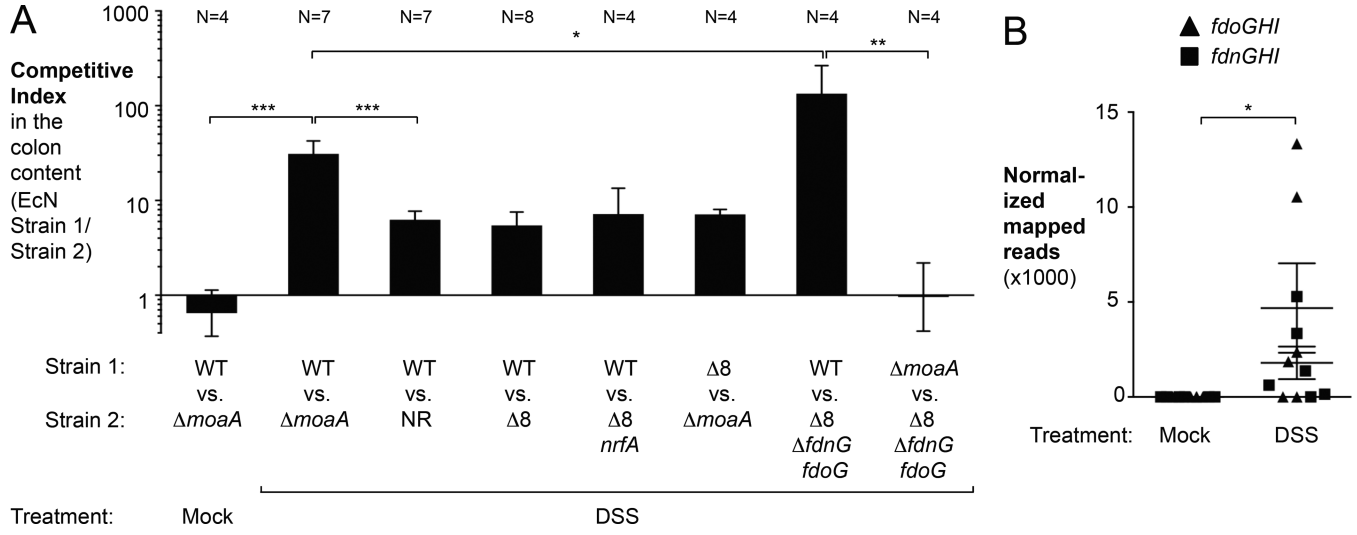

Figure 3. Contribution of anaerobic respiratory pathways to fitness of *E. coli* during DSS-induced inflammation

(A) 3 % DSS-or mock-treated SPF C57BL/6 mice were intragastrically inoculated with an equal mixture of the indicated strains. Five days after inoculation, abundance of each strain was determined and the ratio (competitive index) of the two strains calculated (see also Figure S4A). Bars represent geometric means ± standard error. The number of mice per group (N) is indicated above each bar. (B) Paired end reads from the metagenomic sequencing experiment in Figure 1 were mapped to a non-redundant dataset of representative *fdo* (triangles) and *fdn* (squares) operons. Each symbol represents one animal (N = 6 per treatment group). The lines show the geometric mean ± standard error. *, $P < 0.05$, **, $P < 0.01$; ***, $P < 0.001$.

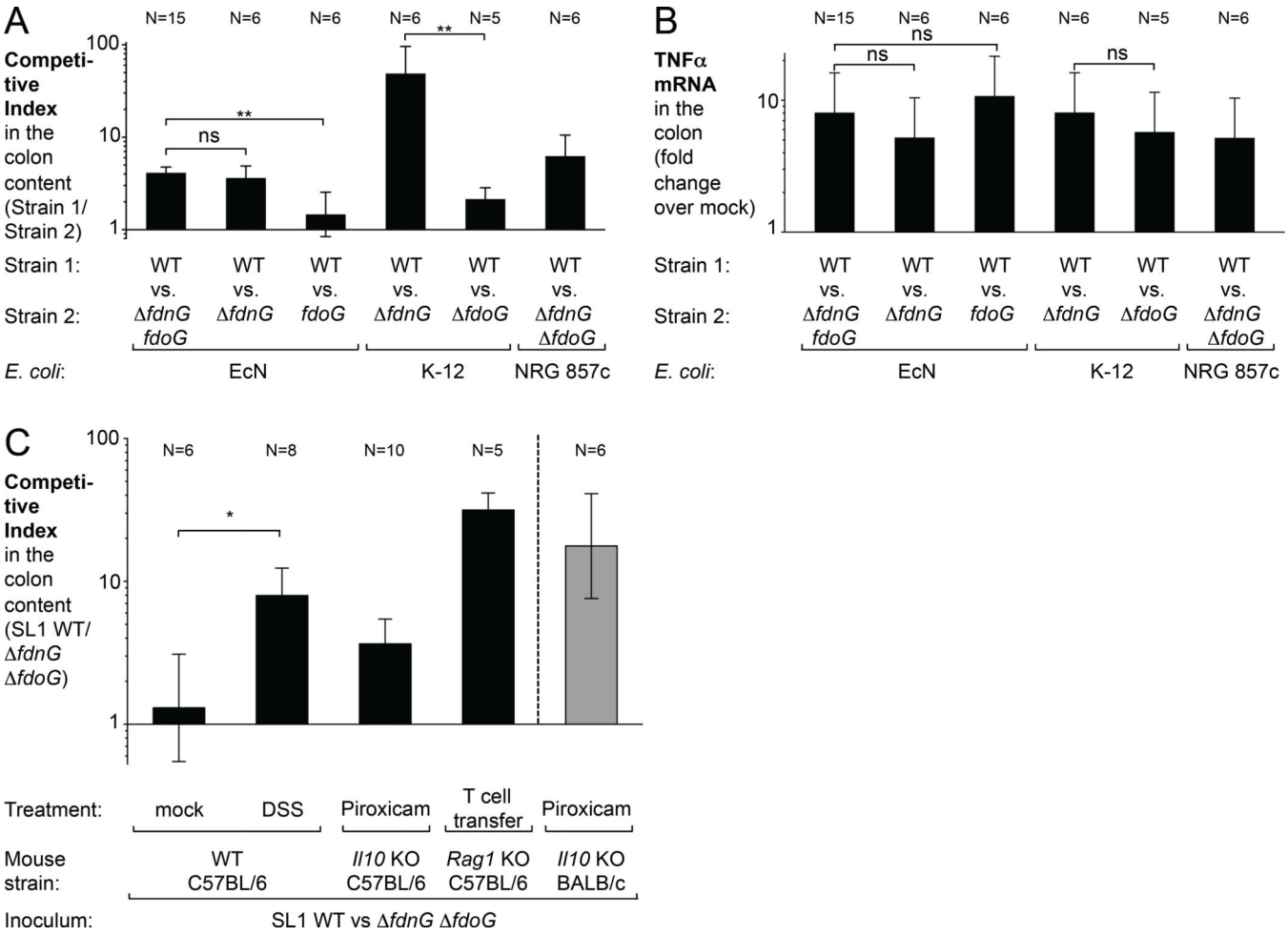

Figure 4. Formate dehydrogenases enhance growth of *E. coli* in the inflamed gut

(A-B) SPF C57BL/6 mice, treated with 3 % DSS for 4 days, were intragastrically inoculated with an equal mixture of the indicated *E. coli* wild-type (WT) strains and isogenic mutants. (A) Competitive index in the colon content five days after inoculation (see also Figure S5C). (B) mRNA levels of *Tnfa* in the colon tissue were determined by RT-qPCR. (C) Competitive index in the colon content. SPF mice with different models of murine colitis were intragastrically inoculated with a mouse commensal *E. coli* strain (SL1). Mice received an equal mixture of WT and the isogenic Δ*fdnG* Δ*fdoG* mutant. Wild-type C57BL/6 mice were mock-or DSS-treated (2 %) and colonized for 9 days. *Il10* knockout (KO) C57BL/6 mice were treated with piroxicam 2 days prior to colonization and colonized for 7 days. *Rag1* KO mice on a C57BL/6 background received a T cell transfer, and after developing signs of inflammation were colonized for 9 days (see also Figure S6A and B). *Il10* KO BALB/c mice were treated with piroxicam 2 days prior to colonization and were colonized for 14 days (gray bar).

Bars represent geometric means ± standard error. The number of mice per group (N) is indicated in each panel. *, $P < 0.05$, **, $P < 0.01$; ***, $P < 0.001$; ns, not statistically significant.

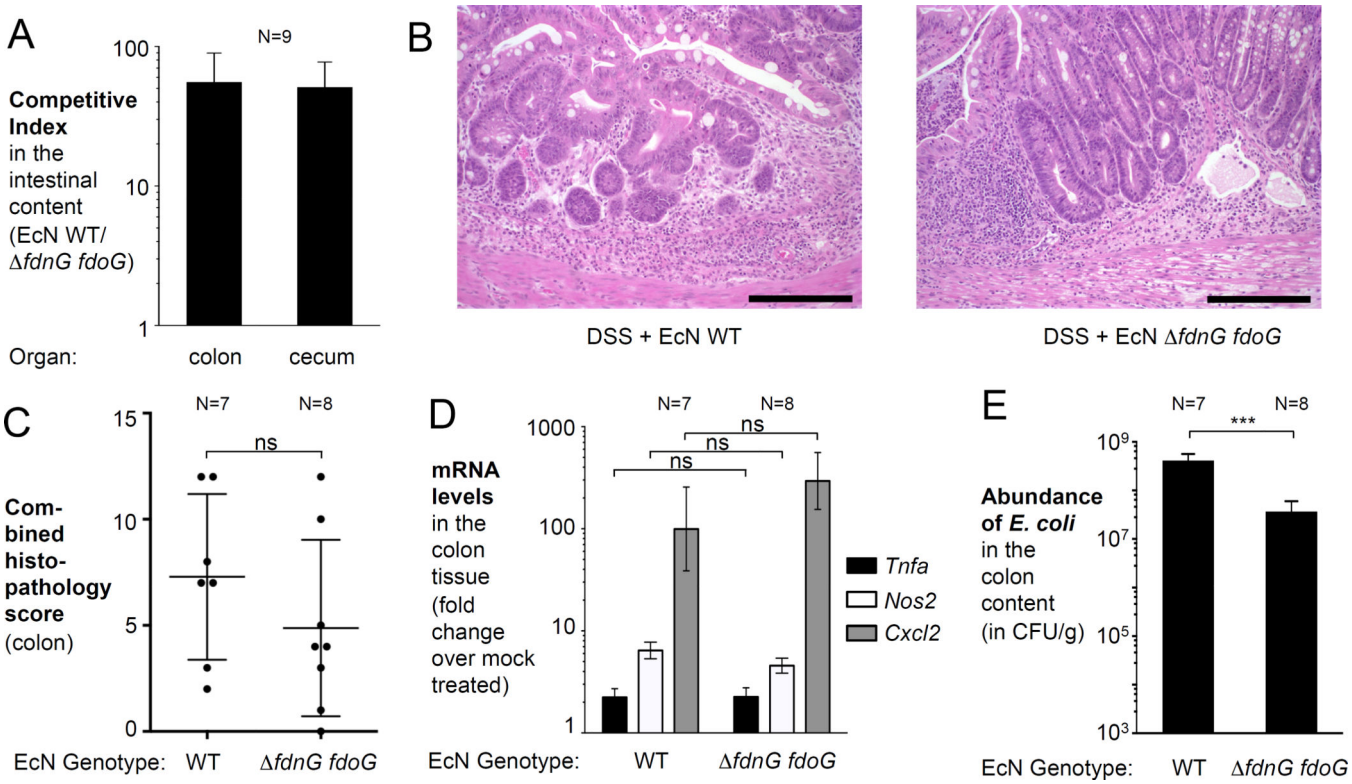

Figure 5. Formate oxidation contributes to the expansion of the *E. coli* population during colitis

(A) SPF C57BL/6 mice were pre-colonized with an equal mixture of the *E. coli* Nissle 1917 (EcN) wild-type strain (WT) and the isogenic Δ*fdnG fdoG* mutant. Inflammation was induced by 3 % DSS treatment for 9 days and the competitive index in the cecum and colon determined. (B – E) Groups of SPF animals were pre-colonized with either the EcN WT or the Δ*fdnG fdoG* mutant and inflammation induced for 9 days by administration of 3 % DSS. (B) Representative images of hematoxylin and eosin-stained sections of the colon. Scale bar, 200 μm. (C) Combined histopathology score of lesions in the colon. Lines represent the mean ± standard deviation. (D) mRNA levels of pro-inflammatory markers (*Tnfa*, black bars; *Nos2*, white bars; *Cxcl2*, gray bars) as determined by RT-qPCR. (E) Abundance of the experimentally introduced *E. coli* strains in the colon content (see also Figure S7B). Bars represent geometric means ± standard error. The number of mice per group (N) is indicated in each panel. *, $P < 0.05$, **, $P < 0.01$; ***, $P < 0.001$; ns, not statistically significant.

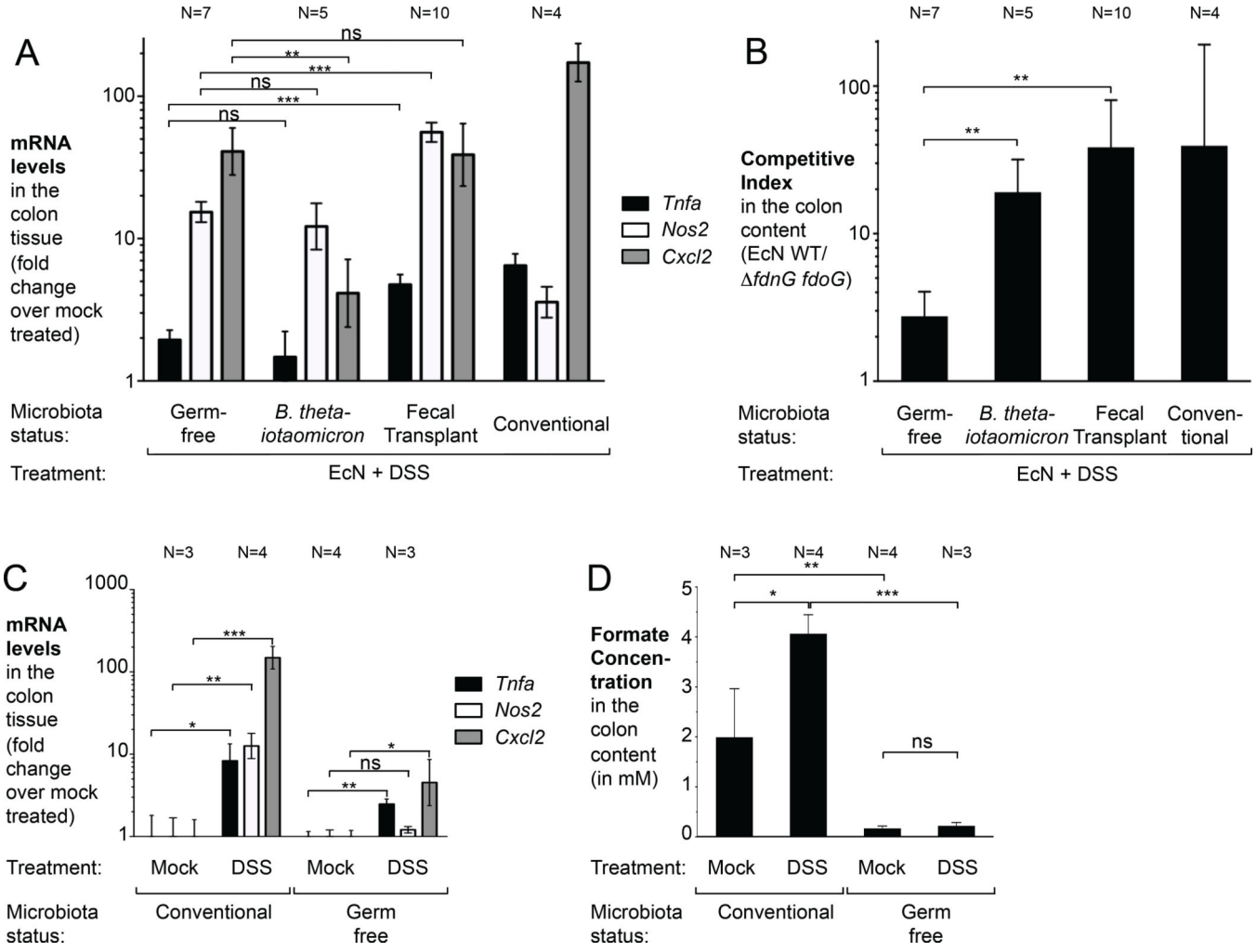

Figure 6. Formate in the intestinal lumen is microbiota-derived

(A and B) Germ-free Swiss Webster mice were pre-colonized for three days with *E. coli* alone, *E. coli* and *B. thetaiotaomicron* or *E. coli* and a fecal transplant from a healthy, conventionally raised mouse. The *E. coli* inoculum consisted of an equal mixture of the *E. coli* Nissle 1917 (EcN) wild-type strain (WT) and the Δ*fdnG fdoG* mutant. Inflammation was induced by 3 % DSS. Conventional SPF Swiss Webster mice received 3 % DSS and an equal mixture of EcN WT and the .*fdnG fdoG* mutant. Samples were analyzed 9 days after the start of DSS treatment (see also Figure S7B). (A) mRNA levels of the pro-inflammatory markers (*Tnfa*, black bars; *Nos2*, white bars; *Cxcl2*; gray bars) as determined by RT-qPCR. (B) Competitive index of the EcN WT and the Δ*fdnG fdoG* mutant. (C and D) Conventionally raised SPF and germ-free C57BL/6 mice were treated with 2 % DSS or mock-treated for 7 days. (C) mRNA levels of the pro-inflammatory markers (*Tnfa*, black bars; *Nos2*, white bars; *Cxcl2*; gray bars) as determined by RT-qPCR. (D) Extracellular formate levels in the lumen of the colon as determined by GC/MS.

Bars represent geometric means ± standard error. The number of mice per group N) is indicated above each bar. *, $P < 0.05$; **, $P < 0.01$; ***, $P < 0.001$; ns, not statistically significant.

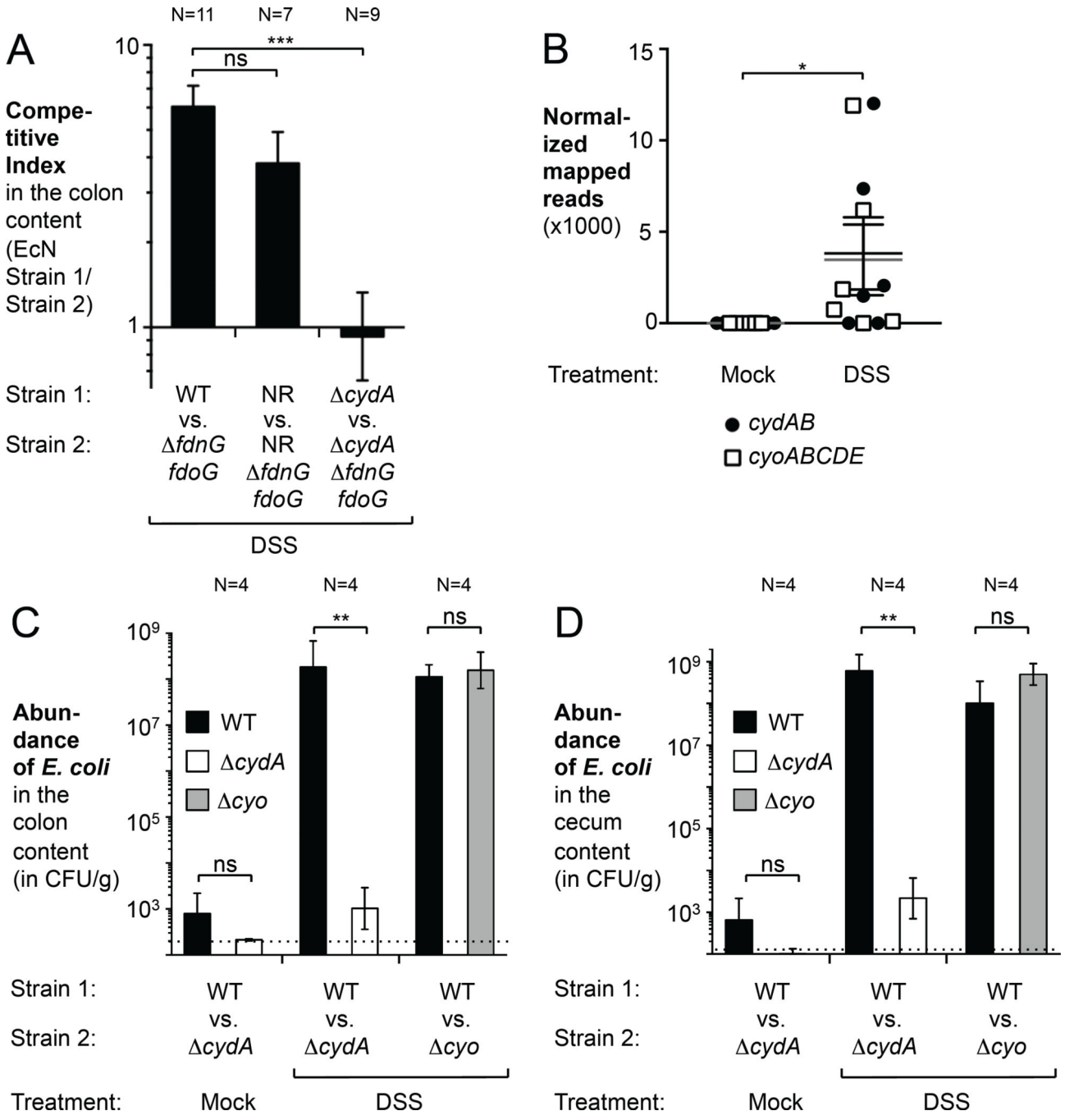

Figure 7. Utilization of oxygen by *E. coli* in the DSS colitis model

(A) Groups of SPF C57BL/6 mice, treated with 3 % DSS for 4 days, were inoculated with the indicated strains. The competitive index of the EcN strains was determined in the colon content after 5 days (see also Figure S7F). (B) Sequencing reads from the metagenomics data set were mapped to representative *cydAB* (black circles and lines) and *cyoABCDE* (white squares and gray lines) operons. Each symbol represents one animal. Lines show the mean ± standard deviation. (C and D) Groups of SPF C57BL/6 mice were treated for 4 days with 3 % DSS. Animals were intragastrically inoculated with an equal mixture of the EcN

wild-type (WT; black bars) and the Δ*cydA* mutant (white bars) or the EcN WT and the Δ*cyoABCD* (Δ*cyo;* gray bar) mutant. The population of each strain after 5 days in the colon (C) and cecum (D) is shown.

Bars represent geometric means ± standard error. The number of mice used (N) is indicated in each panel. *, $P < 0.05$; **, $P < 0.01$; ***, $P < 0.001$; ns, not statistically significant.